

Free vibrations of precast modular steel-concrete composite railway track slabs

Stephen Kimindiri Kimani ^{1a} and Sakdirat Kaewunruen ^{*2}

¹ Department of Civil Engineering, School of Engineering, University of Birmingham, Birmingham B15 2TT, UK

² Birmingham Centre for Railway Research and Education, School of Engineering, University of Birmingham, Birmingham B15 2TT, UK

(Received January 05, 2017, Revised March 14, 2017, Accepted March 15, 2017)

Abstract. This paper highlights a study undertaken on the free vibration of a precast steel-concrete composite slab panel for track support. The steel-concrete composite slab track is an evolution from the slab track, a form of ballastless track which is becoming increasingly attractive to asset owners as they seek to reduce lifecycle costs and deal with increasing rail traffic speeds. The slender nature of the slab panel due to its reduced depth of construction makes it susceptible to vibration problems. The aim of the study is driven by the need to address the limited research available to date on the dynamic behaviour of steel-concrete composite slab panels for track support. Free vibration analysis of the track slab has been carried out using ABAQUS. Both eigenfrequencies and eigenmodes have been extracted using the Lanczos method. The fundamental natural frequencies of the slab panel have been identified together with corresponding mode shapes. To investigate the sensitivity of the natural frequencies and mode shapes, parametric studies have been established, considering concrete strength and mass and steel's modulus of elasticity. This study is the world first to observe crossover phenomena that result in the inversion of the natural orders without interaction. It also reveals that replacement of the steel with aluminium or carbon fibre sheeting can only marginally reduce the natural frequencies of the slab panel.

Keywords: free vibration; steel-concrete composite; ballastless track; slab panel track; natural frequency; natural mode; mass; stiffness; crossover; veering

1. Introduction

This paper focuses on the study undertaken on the free vibrations of a precast steel-concrete composite slab panel for track support developed by Griffin (2013). The slab panel track is a form of ballastless track system. An increase in train speed and axle loading and problems facing conventional ballasted track systems in the last 40 years gave rise to ballastless track systems (Michas 2012). The problems associated with ballasted track systems are; the increased speeds and daily movements of high-speed services has resulted in significant degradation of the systems (Matias 2015); movements of the system during loading translates to energy leading to degradation of the ballast and track quality hence increased need for maintenance (Bezin and Farrington 2010); Low design life compared to other systems (Britpave 2016) and scarcity of high-quality ballast material (Peng *et al.* 2012). Though not an issue limited to ballasted tracks only, susceptibility of timber sleepers to both biological and mechanical deteriora-

tion is a problem with these systems (Manalo *et al.* 2010). In addition to overcoming the demerits of a ballasted track system described above, other justifications for a ballastless track are; need for track which is accessible to road vehicles; reduced track noise and vibration requirements; avoid environmental pollution by release of dust from ballast; reduced height of construction and reduced maintenance requirements and therefore higher track availability (Esveld 1997). According to Robertson *et al.* (2015), growing economic pressure is pushing railway asset owners worldwide to reduce their life cycle costs hence ballastless track systems are becoming more attractive compared to ballasted tracks. In addition, increasing speeds and need for large operational windows to meet the growing interest in mixed passenger-freight lines make a ballastless track attractive over ballasted tracks.

The aim of the study is to determine the free vibration of the precast steel-concrete composite slab panel for track support by using finite element (FE) method. Based on the literature review undertaken for the study, very limited information is currently available on the vibration behaviour of steel-concrete composite slab panel for track support. This study aims to bridge that gap and provide new findings to improve railway vibration control methods. The understanding into natural frequencies can enable an improved design to cater high frequency vibrations from trains. Steel-concrete composite slab panel for track support is currently being considered in the replacement of ageing deck elements in steel-girder railway bridges as it provides

*Corresponding author, Senior Lecturer, Ph.D., MBA, MIEAust, CPEng, NER, RPEQ, FHEA, Visiting BRIDGE Professor at the University of Illinois at Urbana Champaign, USA, E-mail: s.kaewunruen@bham.ac.uk

^a Formerly Masters Student, E-mail: kimindiri2000@yahoo.com

slim deck construction offering savings in dead load and improved durability (Griffin *et al.* 2014, 2015). The slender construction and the one-way spanning nature of the panel make it vulnerable to vibration problems (De Silva and Thambiratnam 2011, Altoubat *et al.* 2015, Hou *et al.* 2015).

The technology of the steel-concrete composite slab panel track has developed as an improvement to concrete slab tracks. This type of slab track is much suited for the replacement of deck and track elements in existing railway bridges (Griffin 2013). According to Choi *et al.* (2010) timber track steel plate girder bridges have been in use for many years now, and over time, the bridges have deteriorated due to corrosion, abrasion, cracking and deformation of members. This has led to a decline in structural safety and durability. Growth in passenger numbers and freights, changes in design loads and environmental conditions have all exacerbated the condition of these bridges. Choi *et al.* (2010) have identified the following major problems associated with timber tracks on steel plate girder bridges:

- Long-term degradation of impact absorption due to vulnerability to train impact loads.
- Frequent need of replacement of track components.
- More than necessary maintenance effort due to the high proportion (50% - 60%) of maintenance work being replacement of the tie plates and sleepers only.
- Track insulation resistance elements degradation due to exposure to rain.

Replacement of the timber track on these bridges needs developing an innovative type of ballastless track to cope with the following construction constraints as identified by Choi *et al.* (2010) and Griffin *et al.* (2014); maintaining same track levels before and after track replacement; narrow windows for construction for operational tracks; limitations in the steel girder strength; low clearances for platforms and tracks and inadequate widths at structures. A number of researchers have developed solutions to cope with the above challenges. Choi *et al.* (2010) developed a precast steel-concrete composite slab panel (PSP) track with the objective of improving long-term workability and durability of the existing bridges in order to enhance performance of railway lines. Griffin (2013) and Griffin *et al.* (2014, 2015) researched on a theoretical design solution of a precast steel-concrete composite slab panel to replace the existing timber track on the Sydney Harbour Bridge as shown in Fig. 1.

Other types of steel-concrete composite slab track that have been developed include the steel girder-precast concrete slab track developed by Sugimoto *et al.* (2013). In the field of highway bridges, Kim and Jeong (2006, 2009 and 2010) proposed use of a profiled steel sheeting with perfobond ribs as participating formwork for box girder composite deck construction. Relevant research work to composite slab decks was undertaken by Shim *et al.* (2001) to investigate the headed shear studs shear capacity in composite precast concrete slab-steel girders for road bridges. The steel-concrete composite precast slab panel developed by Griffin (2013) comprised of a minimum 0.18 m deep composite slab with a 1 mm thick BONDEK II

profiled steel sheeting. The overall length of the slab was 3.237 m. The panel sections within 0.616 m from both ends were locally thickened to 0.23 m deep to resist hogging moments due to derailment loads. The panel acts compositely with the supporting pair of steel girders and spans 2.205 m measured from the centre lines of the steel girders. Composite action between the panel and the supporting steel girders was achieved via two rows x 3 columns of headed shear studs welded to the top flanges through the profiled steel sheeting at the flange locations. Shear reinforcement was provided in form of 10 mm diameter link bars as follows; 12 no. links at 0.13 m centre-to-centre spacing were provided for the 0.18 m deep section and 4 no. links at 0.1 m centre-to-centre spacing were provided for the 0.23 m deep section of the panel. Details of the composite precast slab are shown on Fig. 1 and the material properties are summarized in Table 1 below.

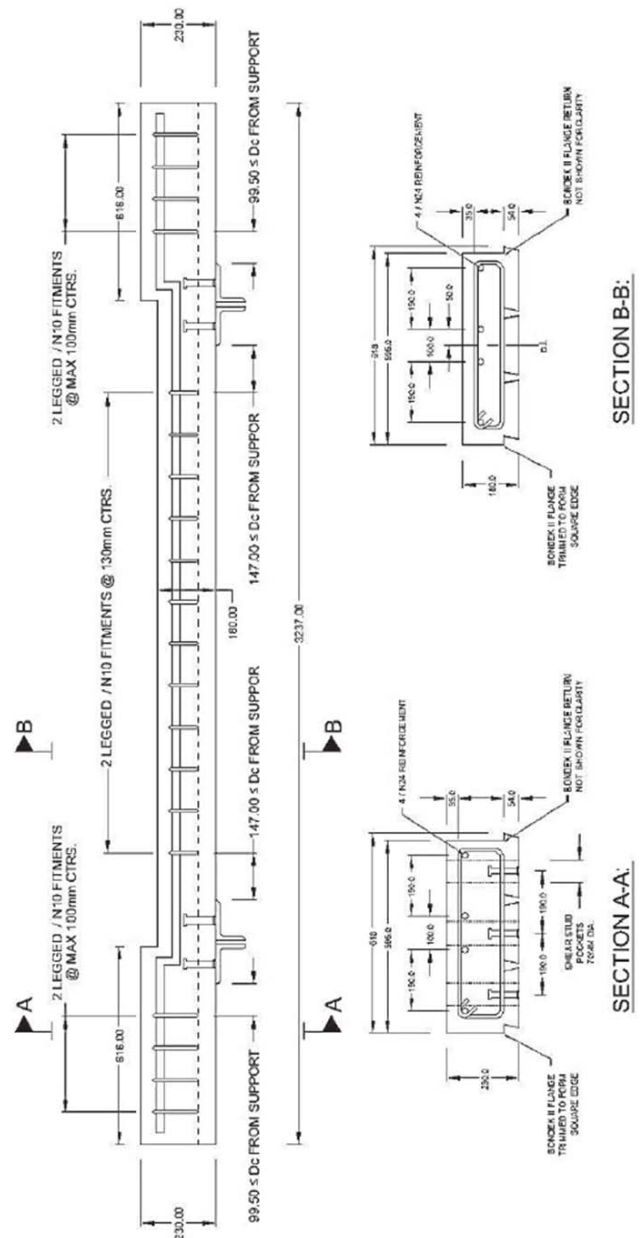


Fig. 1 Modular panel for track slabs

Table 1 Precast steel-concrete composite slab panel materials properties

Material	Properties
Concrete	28 days cube strength, $f'c$: 50 N/mm ²
	Short-term modulus of elasticity: 34652 N/mm ²
	Poisson ratio: 0.2
	Mass: 2400 Kg/m ³
Profiled steel sheeting (High Tensile Steel Bondek II profile manufactured by BHP Building Products)	Yield stress: 550 N/mm ²
	Thickness: 1.0 mm
	Modulus of Elasticity: 200000 N/mm ²
	Poisson ratio: 0.3
Tensile and shear steel reinforcement (D500N grade)	Yield stress: 500 N/mm ²
	Modulus of Elasticity: 200000 N/mm ²
	Poisson ratio: 0.3
Shear studs	Yield stress: 420 N/mm ²
	Modulus of Elasticity: 200000 N/mm ²
	Poisson ratio: 0.3
Supporting steel girders	Yield stress: 300 N/mm ²
	Modulus of Elasticity: 200000 N/mm ²
	Poisson ratio: 0.3

2. Previous research

According to Smith *et al.* (2009), the solutions to the vibration problems of continuous systems can be generally found using integration of continuous functions. However, according to Chopra (2011), due to the infinite number of degrees of freedoms for continuous systems, their analysis is not feasible for practical structures. Due to the simplicity of the matrices methods used for MDOF systems, techniques are available that discretize one-dimensional continuous systems (e.g., beam in transverse vibration only) to allow their solutions to be found using matrices methods. As a result, a system of ordinary differential equations, as many as the DOFs required, replaces the governing partial differential equation of the one-dimensional continuous system. The two methods available for discretizing are the Rayleigh-Ritz and the Finite Element methods (Chopra 2011). The Finite Element (FE) analysis is the most common of these techniques (Smith *et al.* 2009).

According to Chopra (2011), the formulation of the finite element method governing equations for one-dimensional continuous systems can be extended to two and three-dimensional continuous systems. With decreasing element size, and for properly formulated finite elements, the results converge to the exact solution and the larger the number of finite elements the more accurate will be the solution. As opposed to one-dimensional finite elements, compatibility at the finite element nodes for the two and three-dimensional continuous systems does not necessarily lead to compatibility across the element boundaries and this may result in discontinuities between the elements. Interpolation functions over the finite elements are assumed in a way that the common boundaries will deform together

hence avoiding such discontinuities. Such finite elements are termed as compatible elements (Chopra 2011, Ding *et al.* 2014, Kar and Panda 2015, Attia *et al.* 2015, Moon *et al.* 2015). According to Dassault (2012), for a finite element model, the eigenproblem for natural modes of small vibration can be expressed in classical matrix form as

$$(\mu^2 [M] + \mu [C] + [K]) \{\phi\} = 0 \quad (1)$$

where $[M]$ is the symmetric and positive definite mass matrix; $[C]$ is the damping matrix; $[K]$ is the stiffness matrix; μ is the eigenvalue and $\{\phi\}$ is the eigenvector – the mode of vibration.

The solution to Eq. (1) will have complex eigenvalues and eigenvectors. To obtain a solution with real squared eigenvalues μ^2 , and real eigenvectors only, Eq. (2) can be symmetrized by assuming that $[K]$ is symmetric and by neglecting $[C]$ during the eigenvalue extraction. By assuming further that $[K]$ is positive semi-definite, then μ becomes an imaginary eigenvalue $\mu = iw$ where w is the circular frequency. The eigenproblem can therefore be expressed as

$$(-w^2 [M] + [K]) \{\phi\} = 0 \quad (2)$$

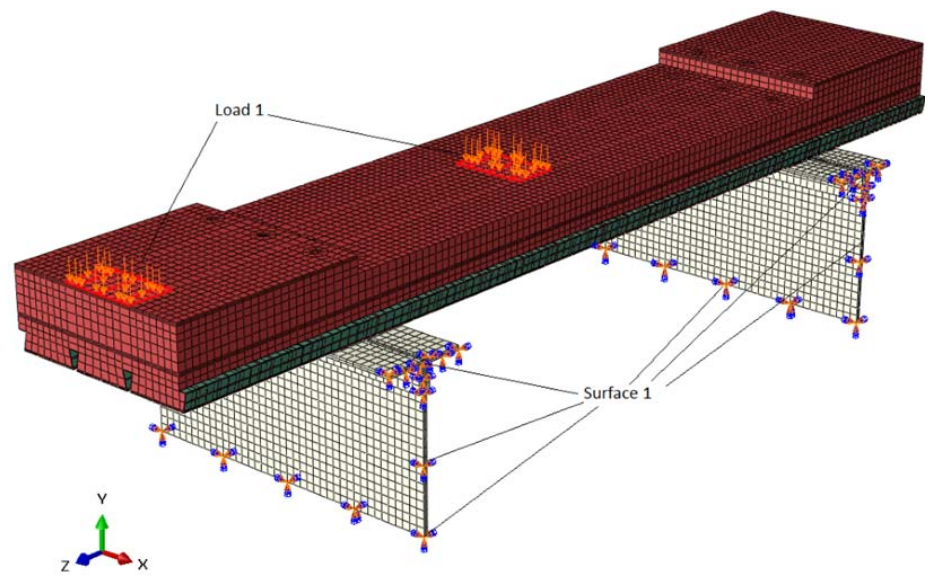
As mentioned earlier, Choi *et al.* (2010); Griffin (2013); Sugimoto *et al.* (2013); Kim and Jeong (2006, 2009 and 2010) and Shim *et al.* (2001) have all developed solutions for steel-concrete composite slab panel deck, however, none of the researchers have undertaken work on the dynamic behaviour of the composite slab decks proposed. Choi *et al.* (2010) have investigated the dynamic behaviour of a steel plate girder for a bridge specimen comprising of a steel-concrete composite precast slab panel track deck simply supported on a pair of steel plate girders. The reasonable conclusion made is that limited literature is currently available on the free vibration of the steel-concrete composite slab panel for track support. The steel-concrete composite technology is however quite common in the building sector for the construction of profiled steel decking-concrete composite floors. Several researchers, among them De Silva and Thambiratnam (2011); Feldmann *et al.* (2009); Venghiac and D'Mello (2010); El-Dardiry and Ji (2006) and Mello *et al.* (2008) have investigated the dynamic behaviour of profiled steel sheeting-concrete composite floor slabs and therefore relevant aspects of their works to the free vibration of the steel-concrete composite slab panel were reviewed for this study.

De Silva and Thambiratnam (2011) investigated the vibration characteristics of a profiled steel sheeting-concrete composite multi-panel floor slab using FE analysis in ABAQUS/Standard. The floor system comprised of a 0.15m deep composite floor slab with 1mm thick profiled steel sheeting which is similar in construction to the precast composite slab panel used in Griffin (2013) study. However, the FE modelling approach adopted by De Silva and Thambiratnam (2011) differed from Griffin (2013) as the floor slab was modelled as follows; the concrete slab was modelled as 3D solid elements (3S6); the profiled steel sheeting was modelled as shell elements (S4R5) and the interface between the steel sheeting and the concrete slab

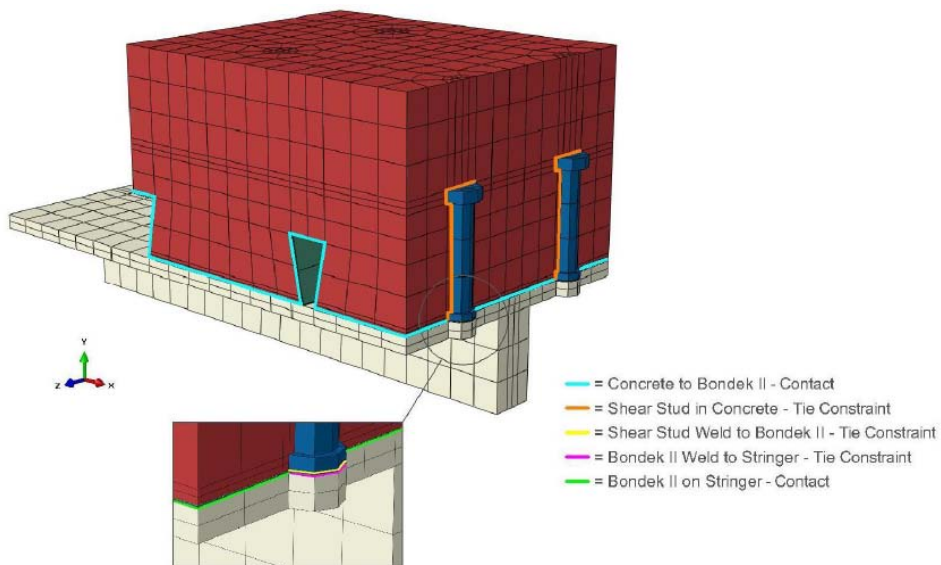
was modelled as full interaction with no slip between the two materials. According to Dassault (2012), for FE modelling incorporating contacts, accuracy issues may arise when using shell elements compared to solid elements. Unlike Griffin (2013) panel which is a single panel supported on a pair of steel girders, De Silva and Thambiratnam (2011) multi-panels were part of a larger floor system comprising of primary and secondary steel beams and columns. This would indicate that the natural frequencies and mode shapes of the two systems would be quite dissimilar due to the difference in boundary conditions, floor mass activated in each mode and stiffness of the floor systems.

El-Dardiry and Ji (2006) carried out work on the modelling of dynamic behaviour of profiled steel sheeting-concrete slab floors using FE analysis in LUSAS FE program. In addition, they carried out parametric studies to

investigate the effect of the profiled steel sheeting contribution, among other parameters, to the natural frequency of the floor slab system. El-Dardiry and Ji (2006) floor system comprised of a 0.13 m deep composite slab with 0.9 mm thick profiled steel sheeting and this is similar in construction to the slabs used by Griffin (2013) and De Silva and Thambiratnam (2011) in their studies. El-Dardiry and Ji (2006) modelled their concrete slab as 3D solid elements and the profiled steel sheeting as thin shell elements which is similar to the modelling approach adopted by De Silva and Thambiratnam (2011). It is not clear, however, how El-Dardiry and Ji (2006) modelled the contact between the concrete slab and the profiled steel sheeting as this information is not given in their work. El-Dardiry and Ji (2006) study found out that removing the profiled steel sheeting from the composite slab reduced the fundamental natural frequency by approximately 5%. This



(a) Symmetrical half model



(b) Contact and boundary conditions

Fig. 2 FE Model of a critical section of the modular panel for track slabs, adopted from Griffin (2013)

Table 2 Contacts and interactions between composite slab panel materials

Interface	Interface type	Master surface	Slave surface
Reinforcing steel in concrete	Embedded	Reinforcing steel	Concrete
Concrete to Bondek II	Surface to surface contact	Bondek II	Concrete
Shear stud in concrete	Tie constraint	Shear stud	Concrete
Shear stud weld to Bondek II	Tie constraint	Bondek II	Shear stud
Bondek II weld to stringer	Tie constraint	Bondek II	Stringer
Bondek II on stringer	Surface to surface contact	Bondek II	Stringer

was attributed to the decrease in the stiffness of the composite slab (location of sheeting at extreme fibre and elastic stiffness of steel approximately 6-7 times the elastic stiffness of the concrete) with slight reduction in the mass of the system (mass of 0.9 mm thick sheeting negligible relative to mass of concrete).

Venghiac and D'Mello (2010) undertook parametric studies to investigate the effect on the fundamental natural frequency for composite slab panels of varying width:length aspect ratios due to the following influences; thickness of slab and grade of concrete. The floor slab used in their study comprised of a 0.375 m deep composite slab with 1.22 mm thick profiled steel sheeting (deep profile). The composite slab was modelled as an orthotropic plate in Autodesk Robot Structural Analysis FE program. The parametric studies showed that for a given aspect ratio of the slab panel, increasing the grade of the concrete led to an increase in the fundamental natural frequency of the composite slab. This could be attributed to the increase in stiffness of the composite slab with no increase in mass of the system.

Based on this critical review, it can be found that the free vibration behaviors of steel-concrete composite panels have not been fully investigated, even though its resonance can cause premature cracks of track slabs. In fact, the track slabs often expand longitudinally and it is critically important to investigate fully the dynamic behaviors in three dimensions, especially the coupling modes. As a result, this study is new and highly beneficial in predictive track maintenance that can reduce economic and environmental costs.

3. Finite element modelling and its validation

A finite element (FE) model has been developed to represent the modular track slabs as shown in Fig. 2. The FE model has been validated using theoretical studies and sensitivity analyses (Mirza *et al.* 2016). Note that this model has been chosen as part of industry-based research collaboration to develop an alternative track-support

component.

3.1 Material properties

Griffin (2013) modelled the concrete and steel in the slab panel as elastic-plastic materials in his study. The concrete and steel properties for the elastic range are as shown in Table 1 of this paper. The plastic properties are not described herein as this are outside the scope of this study.

3.2 Element type and mesh

The concrete slab, profiled steel sheeting, shear studs and supporting steel girders were modelled as solid, 3dimensional eight node (C3D8R) elements with hourglass control. A description of each of these initials is provided in Griffin (2013). The demerit of reduced integration is that it can lead to 'hourglassing' which is the phenomenon of errors being propagated through the model due to zero stresses and strains being introduced at other nodes. Hourglass control is therefore introduced in order to correct these zero stresses and strains and reduce the errors arising from such phenomenon. The steel reinforcement was modelled as 3-dimensional 2 node truss (T3DR) elements. The 'T' stands for truss family. The truss elements are tension and compression only members and were modelled embedded in the concrete (Griffin 2013).

3.3 Contacts and interactions

Table 2 and Fig. 2 adopted from Griffin (2013) summarize the contacts and interactions between the composite slab panel materials. It is worth noting that the contact between the concrete and the profiled steel sheeting was modelled as a surface-to-surface contact with finite sliding, hard contact in the normal direction and a coefficient of friction of 0.5 in the tangential direction (Griffin 2013). One of the recommendations of this study is to evaluate the sensitivity of the natural frequencies of the slab panel to the variation of this friction coefficient.

3.4 Boundary conditions

The cut edges of the supporting steel girders were assigned encastre boundary conditions i.e., fixity in the 3 degrees of translational freedom and fixity in the 3 degrees of rotational freedom.

3.5 Aspects amended to suit free vibration analysis

The materials were assigned mass properties as follows; concrete was assigned a mass of 2400 Kg/m³ in accordance with Table 3 and steel was assigned a mass of 7850 Kg/m³ in accordance with BS EN 1991-1-1:2002 (British Standards Institution 2002) as Griffin (2013) had not proposed any value for steel.

3.6 Material properties adopted for the parametric studies

The range of concrete strength values was adopted from BS EN 1992-1-1:2004 in Table 3 (British Standards

Table 3 Concrete strength and dynamic modulus of elasticity used in the parametric study

	Concrete strength, $f_{ck,cube}$ (N/mm ²)							
	37	45	50	60	75	95	105	115*
E_{cm} (KN/mm ²)	33	34	35	37	39	42	44	45*
E_{dyn} (KN/mm ²)	36.3	37.4	38.5	40.7	42.9	46.2	48.4	49.5

* Reasonable values assumed for the study

Table 4 Concrete strength and dynamic modulus of elasticity used in the parametric study

Material	Properties
Aluminium	Yield stress: 290 N/mm ²
	Modulus of elasticity: 78500 N/mm ²
	Poisson ratio: 0.325
	Mass: 2750 Kg/m ³
High modulus carbon fibre	Yield stress (tensile/compressive): 350/150 N/mm ²
	Modulus of elasticity (0° and 90°): 85000 N/mm ²
	Poisson ratio: 0.1
	Mass: 1600 Kg/m ³

Institution 2004). The dynamic elastic modulus, E_{dyn} , was determined by factoring the short-term modulus of elasticity, E_{cm} , of the concrete by a value of 1.1 as recommended by Feldmann *et al.* (2009). These values are summarised in Tables 3 and 4. The range of the concrete mass values was adopted from BS EN 206-1:2000 (British Standards Institution 2000) for normal weight concrete. These were 2000 Kg/m³; 2200 Kg/m³; 2400 Kg/m³ and 2600 Kg/m³. Additional arbitrary values of 1000 Kg/m³ and 1500 Kg/m³ were considered to account for emerging trends in using high strength light-weight concrete in structures.

The range of the steel modulus of elasticity, E_s was chosen based on the varying values of E_s provided by British Standards Institution (2005, 1994 and 1995) i.e., BS EN 1993-1-1 gives a value of 210 kN/mm²; BS 5950 part 4

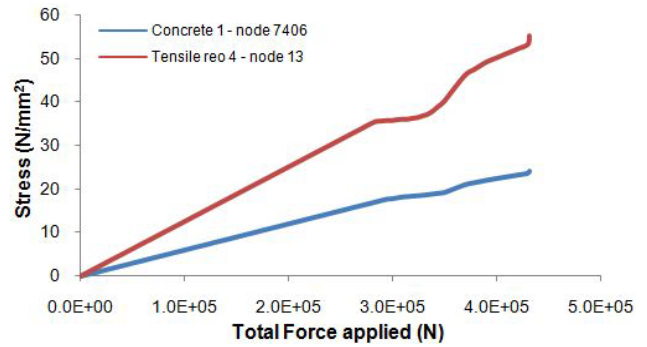


Fig. 4 Model validation stress-load relationship, node 7406 and node 13 in this study

and 6 give values of 205 kN/mm² and 210 KN/mm² respectively and the value of 200 kN/mm² used by Griffin (2013). Additional arbitrary values of 50 kN/mm², 100 kN/mm² and 150 kN/mm² were considered to account for loss of stiffness from corrosion and fire damage. A range of 50 kN/mm² to 215 kN/mm² was therefore adopted for the parametric analysis (Chitra Ganapathi *et al.* 2016, Mashhadi and Saffari 2016, Fang *et al.* 2016).

Values for the material properties adopted for the aluminium and high modulus carbon fibre (HMCF), used as alternative materials to steel sheeting, are summarised in Table 4. The aluminium properties were an arbitrary extract from Tindall (2008)'s Table 1 whilst the HMCF were arbitrarily adopted from ACP Composites (2016).

3.7 Validation of FE model

An abbreviated validation was carried out by undertaking a comparison of Griffin (2013) derailment loading results for selected nodes with results from similar derailment loading. Figs. 3 and 4 show the load-stress relationships of the structure carried out by Griffin (Griffin *et al.* 2014) and by the authors in this study, respectively. The 3-dimensional FE model is deemed to be in very good agreement as the two results were within 5% variation of each other i.e., 55.1 N/mm² for node 7406 and 24.2 N/mm² for node 13.

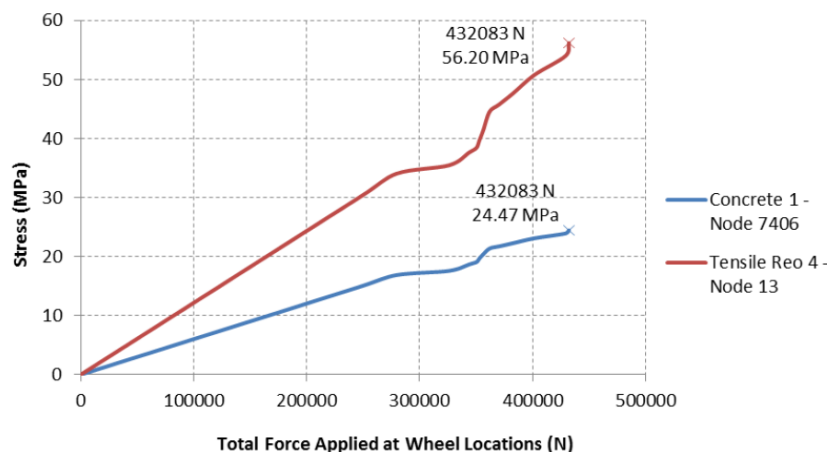


Fig. 3 Model stress-load relationship, node 7406 and node 13 by Griffin (Griffin *et al.* 2014)

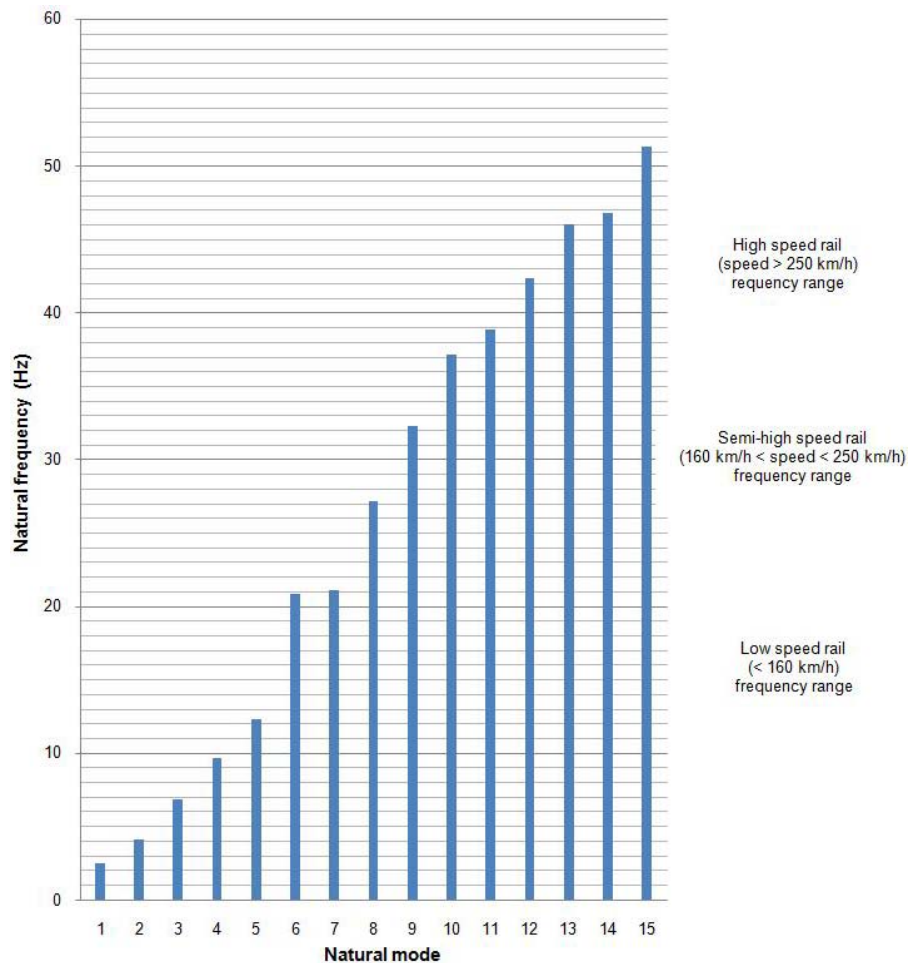


Fig. 5 Natural frequencies and associated modes of vibration of the slab panel, and a correlation of the natural frequencies with typical rail frequency ranges

4. Free vibration analyses

4.1 Natural frequencies and mode shapes

Of the first 500 eigenfrequencies and modes extracted by the Lanczos eigensolver from the free vibration analysis, 15 no. have been identified as being associated with distinctive natural mode shapes (hence considered the first 15 natural modes of vibration) whilst the rest were filtered out as described in the methodology for this study. These natural frequencies of the slab panel and their associated mode shapes are tabulated in Table 5. Fig. 5 below shows these natural frequencies and the associated modes of vibration of the slab panel. The results of the 500 eigenfrequencies extracted by the Lanczos eigensolver are included in Kimani (2016).

4.2 Parametric study of free vibrations

The natural frequencies and associated modes across the concrete strengths range are shown in Fig. 6, which describes the change in natural frequencies of the slab panel across each mode due to the variation in concrete strength. In addition, the effects of steel sheeting stiffness on the natural frequencies and associated modes across are shown Fig. 7. The natural frequencies and associated modes across

the concrete mass range are illustrated in Fig. 8. Fig. 9 below shows the change in natural frequencies where aluminium and carbon fibre sheetings are used as alternative materials to the steel sheeting.

5. Discussions

5.1 Natural frequencies

The fundamental natural frequency of the slab panel was found to be 2.5981 Hz. From the literature review, previous work on dynamic behaviour of a slab panel deck similar to Griffin (2013) was not available. A direct comparison of the results with previous work was therefore not possible. Nonetheless, the fundamental natural frequency of the slab panel was compared with the results of De Silva and Thambiratnam (2011) and, as expected, the value was lower relative to the natural frequency of 4.0 Hz for the 4-panel profiled steel sheeting-concrete slab composite floor slab in their study. This could be attributed to the relatively higher stiffness of the primary beams-secondary beams-composite floor system compared with Griffin (2013) slab panel.

5.2 Changes in natural frequencies

Fig. 5 shows an increase of the natural frequencies with

Table 5 Natural frequencies and associated modes of the slab panel

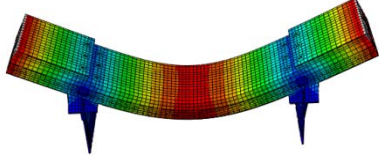
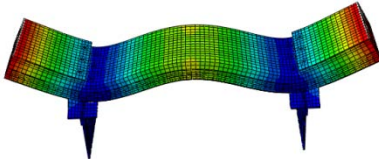
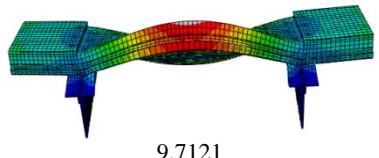
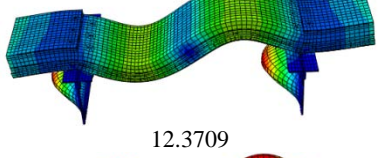
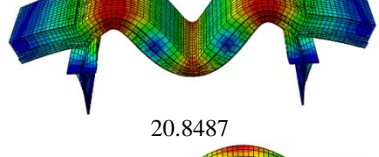
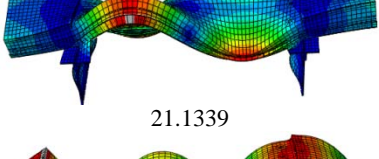
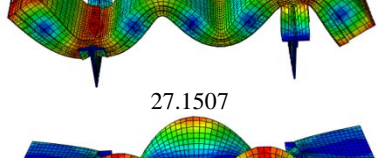
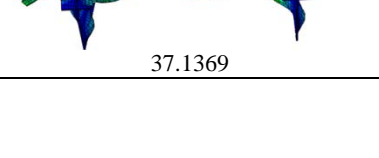
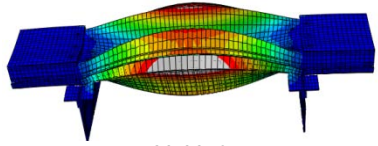
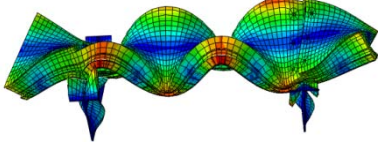
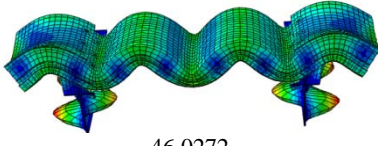
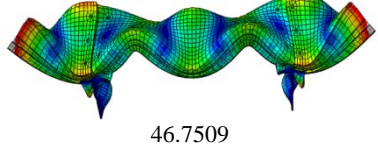
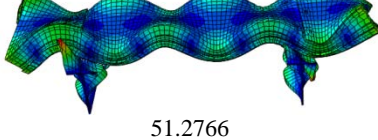
Mode of vibration	Natural frequency (Hz) and corresponding mode shapes
1 st mode - transverse bending	 2.5981
2 nd mode- transverse bending	 4.1649
3 rd mode-transverse bending	 6.8800
4 th mode-torsion	 9.7121
5 th mode-transverse bending	 12.3709
6 th mode -transverse bending	 20.8487
7 th mode-torsion	 21.1339
8 th mode transverse bending	 27.1507
9 th mode- torsion	 32.3012
10 th mode-transverse bending	 37.1369

Table 5 Continued

Mode of vibration	Natural frequency (Hz) and corresponding mode shapes
11 th mode- bi-directional bending	 38.8362
12 th mode-torsion	 42.3631
13 th mode-transverse bending	 46.0272
14 th mode-torsion	 46.7509
15 th mode-torsion	 51.2766

increasing modes of vibration for the slab panel. The slab panel, which is a continuous system was discretized and analysed as a MDOF system. From Eq. (5) below adopted from Chopra (2011), which is the formal non-trivial solution of the matrix eigenvalue problem of an undamped MDOF system, it can be seen that equating the scalar w_n^2 to the stiffness-mass ratio, k/m , means that an increase in the natural frequencies of the slab panel is attributed to the increase in this ratio with each increasing mode of vibration of the system.

$$\det [\mathbf{k} - w_n^2 \mathbf{m}] = 0 \quad (3)$$

As was demonstrated by the parametric studies, varying the k and m of the slab panel resulted in either a decrease or increase of the natural frequencies. Fig. 10 shows the decreasing trend in the generalised mass (see Chopra (2011) for more details) from mode to mode, which goes to show the stiffness-mass ratio increases with increasing modes of vibration.

5.3 Dynamic mode shapes

15 distinctive mode shapes were identified as the natural modes of vibration from the first 500 eigenmodes extracted by the Lanczos eigensolver in ABAQUS/Standard. Higher order eigenmodes (above the 52nd eigenmode) were immediately removed as their mode shapes were not visually distinctive since these were associated with low amplitude vibrations of the concrete slab. Eigenmodes

which were dominated by the vibration of the steel support girders (buckling of the webs and flanges) were filtered out as well as the vibration of the support girders was not part of the study. Coupled eigenmodes were removed as these could not be described as pure modes of vibration of the slab panel. For example, the 8th eigenmode extracted from the Lanczos eigensolver, shown below in Fig. 11, was observed to both twist and bend the slab panel about the minor axis. In addition, eigenmodes with very close eigenfrequencies were identified and the non-dominant ones removed to ensure that only one natural mode was associated with that natural frequency. The fundamental natural mode shape was identified as transverse bending of the slab panel. From Tables 5 and 6, it can be seen that the first 15 natural mode shapes of the slab panel are dominated by the transverse bending (8 modes) and torsion mode shapes (6 modes). This is expected due to the slender and one-way spanning nature of the slab panel. The only other mode shape identified was the bi-directional bending of the slab panel which could be attributed to the reduced depth of the slab in the longitudinal direction due to the profile of the steel sheeting.

A correlation of the natural frequencies of the slab panel with typical rail frequency ranges was made as shown in Fig. 5. The first 7 natural frequencies can be seen to fall within the range of low speed rail frequencies hence resonance damage to the slab panel from low speed rail vibrations is most likely to result from transverse bending of the slab panel. Likewise resonance damage to the slab

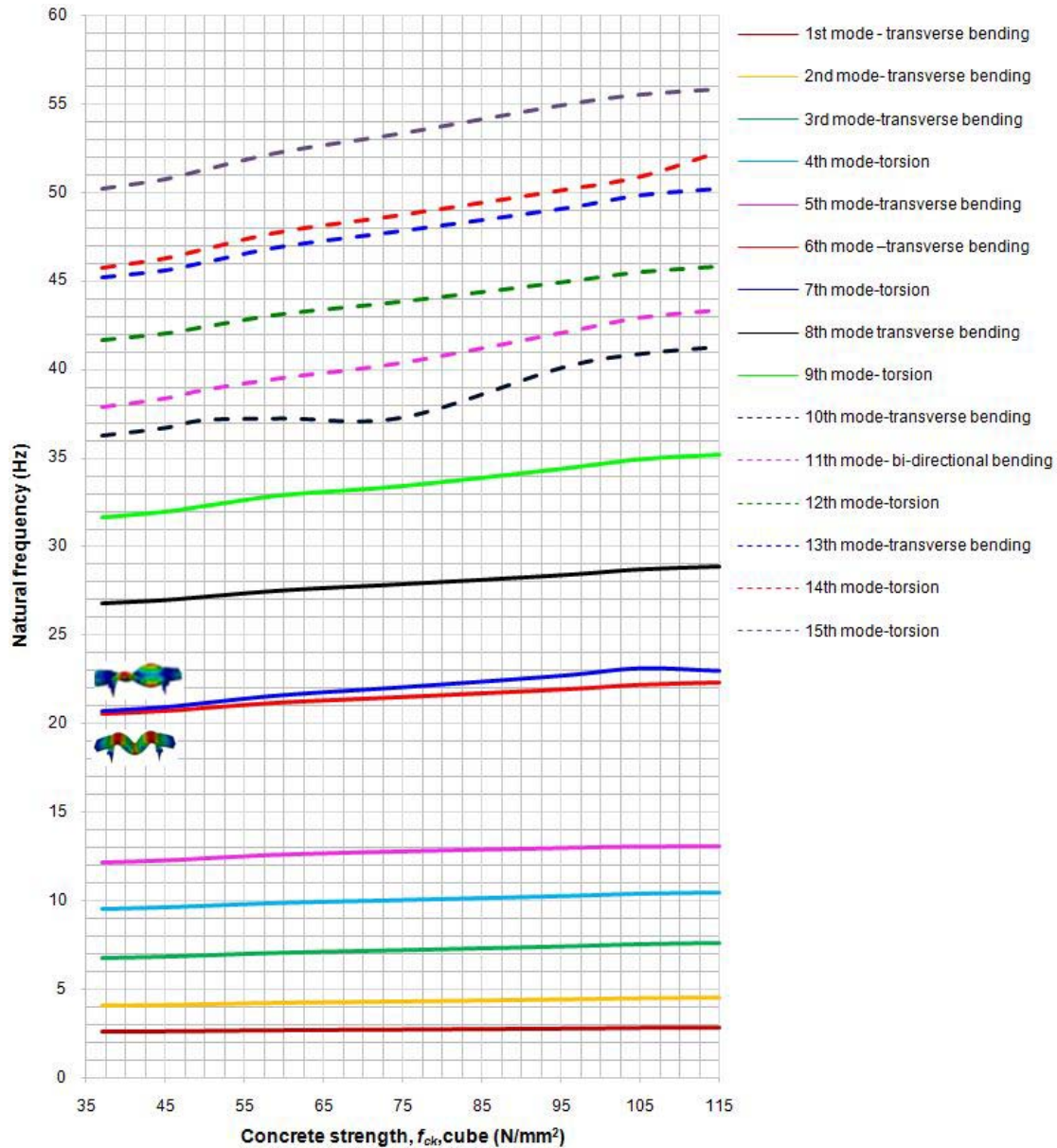


Fig. 6 Natural frequencies of slab panel with variation in concrete strength

panel from semi-high speed and high speed rail vibrations will likely result from transverse bending or torsion of the slab panel as these modes dominate these two ranges.

5.4 Parametric sensitivity

5.4.1 Effect of variation of concrete strength

The effect of varying the strength of the concrete was to vary the stiffness of the system since the concrete strength, per se, has no influence on the stiffness-mass ratio of the system. Fig. 6 shows that increasing the concrete strength results in an increase in the natural frequencies of the slab panel. An increase of 10.1% was observed in the fundamental natural frequency from increasing the concrete strength from 37 N/mm² to 115 N/mm², i.e., a 36.4% increase in the dynamic modulus of elasticity of the concrete. The slopes of the curves for the low order natural modes (modes 1–9) were observed to be generally relatively

flatter compared with the high order natural modes (modes 10–15). This demonstrates that the change of the stiffness-mass ratio with increasing stiffness is much higher in the high order modes. Potential crossover phenomenon was observed between the 6th and the 7th natural mode at a concrete strength of 37 N/mm².

5.4.2 Effect of variation of profiled steel sheeting stiffness

Fig. 7 shows that increasing the stiffness of the steel sheeting results in an increase in the natural frequencies of the slab panel. An increase of 2.9% was observed in the fundamental natural frequency from increasing the modulus of elasticity from 50 KN/mm² to 215 KN/mm², i.e., a 330% increase in the modulus of elasticity of the steel. The slopes of the curves for the low order natural modes (modes 1–8) were observed to be generally relatively flat throughout the stiffness range compared with the high order natural modes

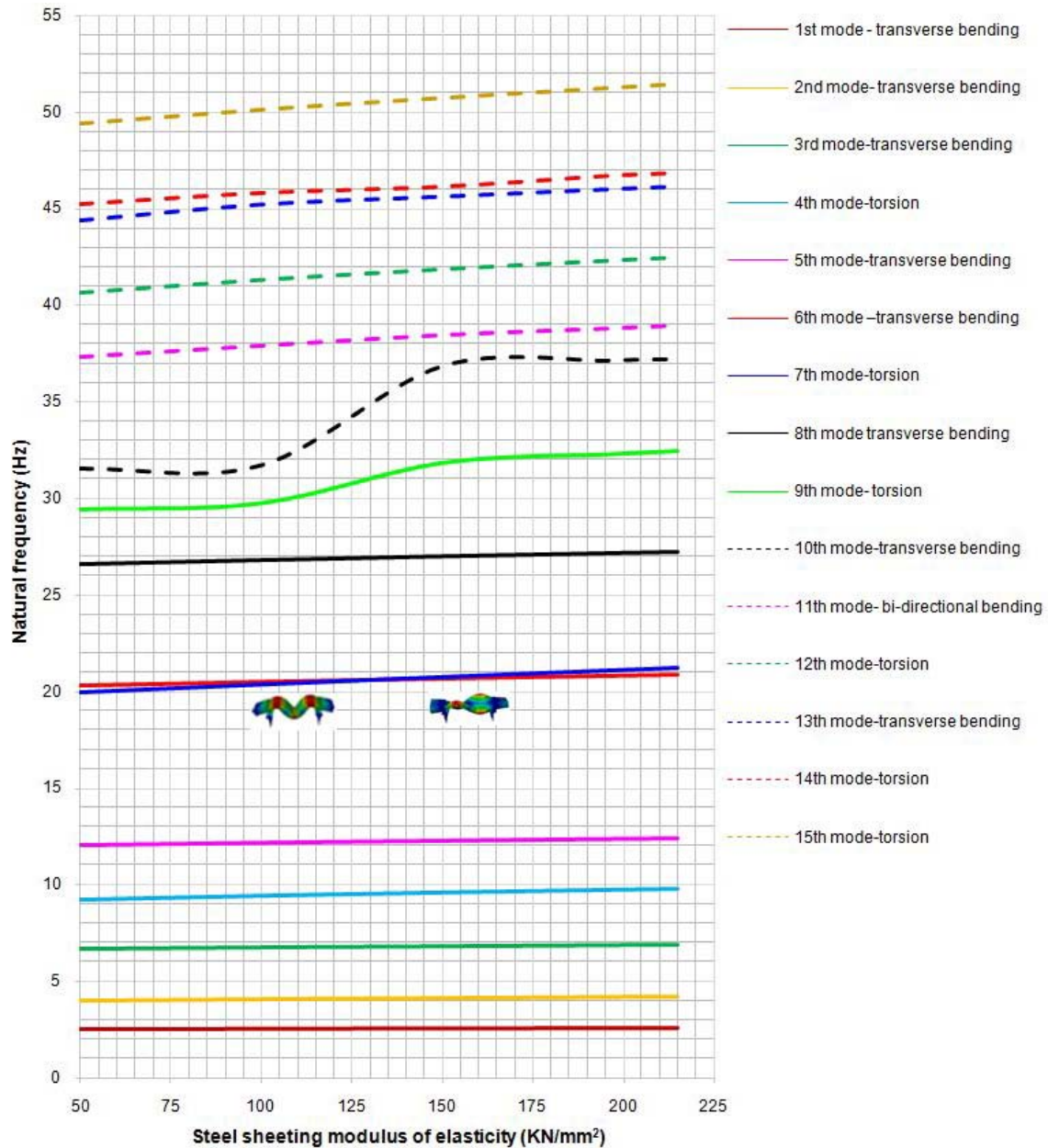


Fig. 7 Natural frequencies of slab panel with variation in profiled steel sheeting stiffness

(modes 11–15). This demonstrates that for the high order natural modes, the change of the stiffness-mass ratio with increasing stiffness is much higher compared to the low order modes. Crossover phenomenon was observed between the 6th and the 7th natural mode at steel modulus of elasticity of approximately 125 KN/mm².

5.4.3 Effect of variation of concrete mass

Fig. 8 shows that increasing the concrete mass results in a decrease in the natural frequencies of the slab panel. A decrease of 33.6% was observed in the fundamental natural frequency from increasing the concrete mass from 1000 Kg/m³ to 2600 Kg/m³, i.e., a 160% increase in the mass of the concrete. The slopes of the curves for the low order natural modes (modes 1–4) were observed to be generally relatively flatter compared with the high order natural modes (modes 6–15). This demonstrates that the change of

the stiffness-mass ratio with increasing concrete mass is much higher in the high order modes. Crossover phenomenon was observed between the 11th and the 13th natural mode at a concrete mass of 1100 Kg/m³ and between the 12th mode and the 13th mode at a concrete mass of approximately 1400 Kg/m³. Potential crossover phenomenon was observed between the 6th and 7th natural modes at a concrete mass of 2600 Kg/m³.

5.4.4 Effect of alternative deck sheeting materials

It is worth noting that the mass and stiffness values for the materials for the study on alternative materials for the steel sheeting were arbitrarily chosen as the study was undertaken with the sole purpose of illustrating the sensitivity of the vibration behaviour of the slab panel to mass and stiffness values outside of the concrete and steel parametric studies (see Fig. 9). The fundamental natural

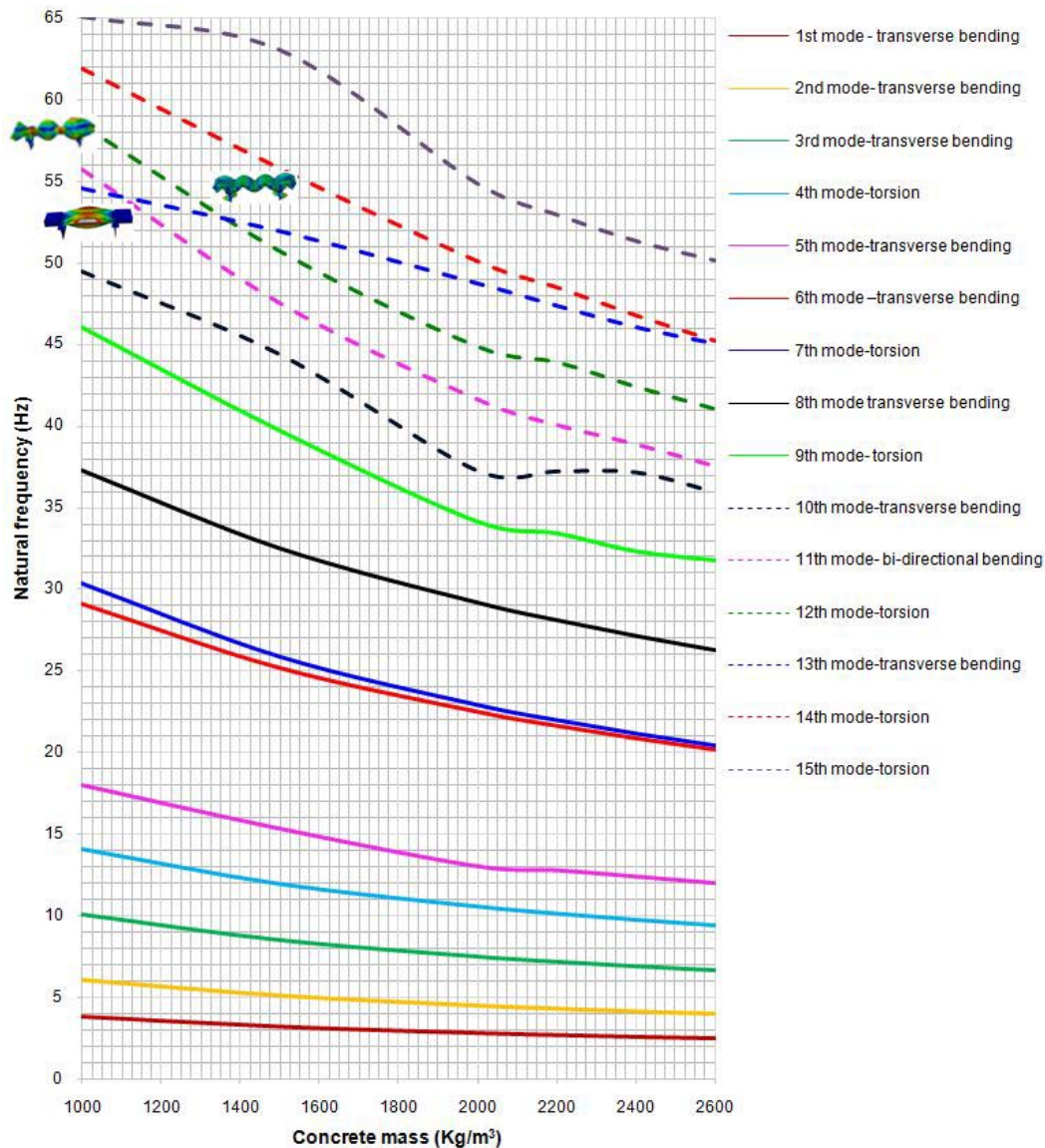


Fig. 8 Natural frequencies of slab panel with variation in mass of the concrete slab

frequency of slab panel with aluminium sheeting was found to be 2.5690 Hz whilst that of the slab panel with carbon fibre sheeting was found to be 2.5784 Hz. Replacing the steel sheeting with aluminium sheeting resulted in a decrease in the fundamental natural frequency of 1.1% whilst replacing with carbon fibre sheeting resulted in a decrease of 0.8%. As the mass and stiffness of these materials vary from steel's, only broad deductions can be made from these observations subject to further studies in this area. The deduction made from this study is that replacing the steel sheeting with aluminium or carbon fibre sheeting results in a very slight change in the natural frequencies of the slab panel, and even though there is a significant reduction in the mass of the sheeting, the overall change in mass of the composite slab is fairly small due to the relatively small cross-section of the sheeting compared with the concrete slab. This means that steel, with the highest stiffness and highest mass of the three materials, resulted in higher natural frequencies compared to the others.

5.7 Crossover phenomena

Crossover phenomenon occurs when two adjacent modes' natural frequencies have their loci, with respect to a change in system parameter (e.g., mass), approach and then cross each other (Perkins and Mote 1986). According to Perkins and Mote Jr. (1986) two converging loci either cross or do not cross each other. Benedettini *et al.* (2009) discussed crossover and veering phenomena as structural damage detection tools. Benedettini *et al.* (2009) observed that the two modes cross each other and invert their natural order without any interaction. In addition, the figure also shows the phenomenon of veering whereby the loci of the two natural frequencies initially approach each and then abruptly diverge without crossing each other (Perkins and Mote 1986).

The crossovers observed in Figs. 6-8 were noted to invert the natural order of the modes without any interaction i.e., the modes retained their mode shapes before and after

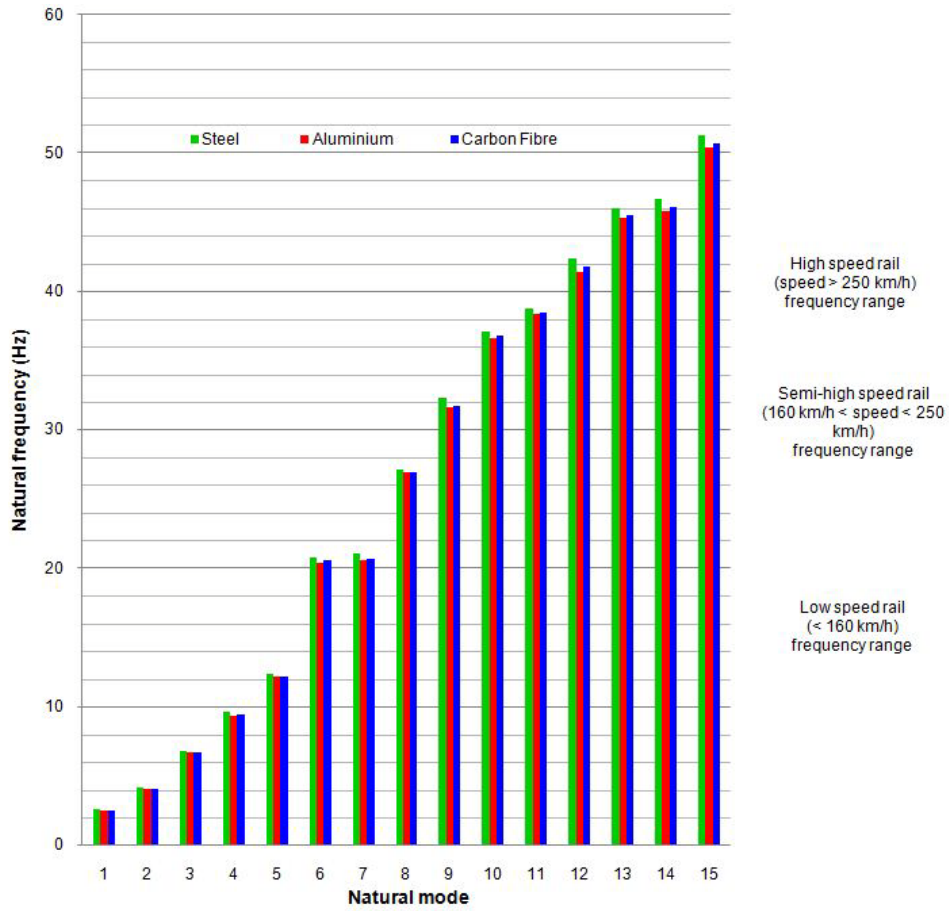


Fig. 9 Natural frequencies of slab panel with aluminium and carbon fibre sheetings as alternatives to steel sheeting, and a correlation of the natural frequencies with typical rail frequency ranges

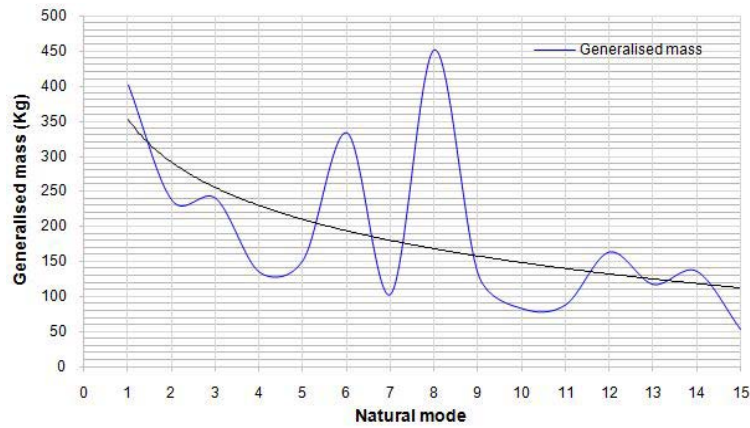


Fig. 10 Variation of system generalized mass with increasing modes

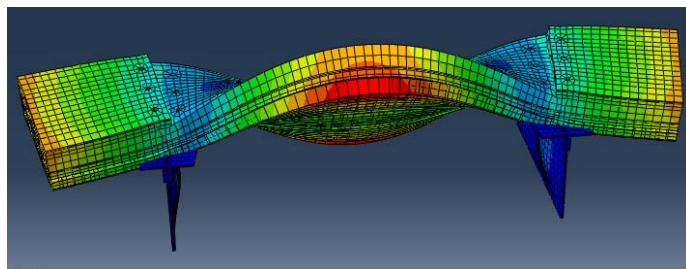


Fig. 11 Coupled torsion and bending about minor axis mode of vibration

the crossover. It is suggested that further studies are undertaken to scrutinize this crossover phenomena, and also any likely veering phenomena as according to Perkins and Mote (1986), two adjacent which may appear to intersect may turn out, when viewed on a larger scale, to be veering. The problem with veering, according to Perkins and Mote (1986), is that the eigenfunctions of the two loci are interchanged rapidly during veering and the two loci interchange paths as well. Observations have been made in the past of curve veering in approximate solutions associated with discretized models. The validity of many approximate solutions has been put in doubt due to the influence of discretization producing curve veering.

6. Conclusions

The fundamental natural frequency of the slab panel was found to be 2.5981 Hz. The fundamental natural mode shape was identified as transverse bending of the slab panel. A correlation of the natural frequencies of the slab panel with typical rail traffic frequency ranges showed that resonance damage from rail traffic vibration would likely result from transverse bending for low speed rail traffic, whilst this type of damage would likely result from both transverse bending and torsion for mid-high speed and high speed rail traffic. We have firstly observed that:

- The effect of variation of the concrete strength on the natural frequencies of the slab panel was found to be an increase in the natural frequencies with increasing strength of the concrete. An increase of 10.1% was observed in the fundamental natural frequency from increasing the concrete strength from 37 N/mm² to 115 N/mm², i.e., a 36.4% increase in the dynamic modulus of elasticity of the concrete.
- By varying the profiled steel sheeting stiffness, the effect on the natural frequencies of the slab panel was found to be an increase in the natural frequencies with increasing stiffness of the steel sheeting. An increase of 2.9% was observed in the fundamental natural frequency from increasing the modulus of elasticity from 50 KN/mm² to 215 KN/mm², i.e., a 330% increase in the modulus of elasticity of the steel.
- The effect of variation of the mass of concrete on the natural frequencies of the slab panel was found to be a decrease in the natural frequencies with increasing concrete mass. Use of alternative deck sheeting materials (aluminium and carbon fibre sheeting) had the effect of lowering the fundamental natural frequency of the slab panel, however the differences were marginal among the three materials.
- The crossover phenomenon observed during the parametric studies resulted in inversion of natural orders without interaction i.e., the modes retained their mode shapes before and after the crossover.

The concluding remarks made were that varying the mass and stiffness changed the dynamic behaviour of the slab panel and subject to further studies, replacing the steel

sheeting with aluminium or carbon fibre would have little effect on the dynamic behaviour of the slab panel. Future studies include the vibration behaviour of a steel-concrete composite slab panel for different track supports and fastening systems. The damped free vibrations have been recently investigated and will appear elsewhere in the near future.

Acknowledgments

Technical assistance and support from Dr Olivia Mirza and Dane Griffin is highly appreciated. The second author would like to gratefully acknowledge the University of Birmingham's BRIDGE Grant, which financially supports his visiting professorship as part of the project "Improving damping and dynamic resistance in concrete through micro- and nano-engineering for sustainable and environmental-friendly applications in railway and other civil construction". This project is part of a collaborative BRIDGE program between the University of Birmingham and the University of Illinois at Urbana Champaign. In addition, the authors are sincerely grateful to the European Commission for the financial sponsorship of the H2020-RISE Project No. 691135 "RISEN: Rail Infrastructure Systems Engineering Network", which enables a global research network that tackles the grand challenge of railway infrastructure resilience and advanced sensing in extreme environments (www.risen2rail.eu).

References

- ACP Composites (2016), High modulus carbon fibre. Available at: <http://www.acpsales.com/home.html> (Accessed on 1st July 2016)
- Altoubat, S., Ousmane, H. and Barakat, S. (2015), "Effect of fibers and welded-wire reinforcements on the diaphragm behavior of composite deck slabs", *Steel Compos. Struct., Int. J.*, **19**(1), 153-171.
- Attia, A., Tounsi, A., Adda Bedia, E.A. and Mahmoud, S.R. (2015), "Free vibration analysis of functionally graded plates with temperature-dependent properties using various four variable refined plate theories", *Steel Compos. Struct., Int. J.*, **18**(1), 187-212.
- Benedettini, F., Zulli, D. and Allagio, R. (2009), "Frequency-veering and mode hybridization in arch bridges", *Proceedings of the IMAC-XXVII*, Orlando, FL, USA, February.
- Bezin, Y. and Farrington, D. (2010), "A structural study of an innovative steel-concrete track structure", *Proceedings of the Institution of Mechanical Engineers, Part F: Journal of Rail and Rapid Transit*, **224**(4), 245-257.
- Bradford, M and Uy, B. (2007), "Composite action of structural steel beams and precast concrete slabs for the flexural strength limit state", *Aust. J. Struct. Eng.*, **7**(2), 123-133.
- Britpave (2016), Why slab track. Available at: <http://www.britpave.org.uk/RailWhyBuild.in> (Accessed 9th July 2016)
- British Standards Institution (1994), BS 5950-4:1994 Structural use of steelwork in building – Part 4: code of practice for design of composite slabs with profiled sheeting; BSI, London, UK.
- British Standards Institution (1995), BS 5950-6:1995 Structural use of steelwork in building Part 6: code of practice for design of light gauge profiled steel sheeting; BSI, London, UK.
- British Standards Institution (2000), BS EN 206-1:2000 Concrete

- Part 1: specification, performance, production and conformity; BSI, London, UK.
- British Standards Institution (2002), BS EN 1991-1-1:2002 Eurocode 1-Actions on structures – Part 1-1: general actions – densities, self-weight, imposed loads for buildings; BSI, London, UK.
- British Standards Institution (2004), BS EN 1992-1-1:2004 Eurocode 2- Design of concrete structures – Part 1-1: general rules and rules for buildings; BSI, London, UK.
- British Standards Institution (2005), BS EN 1993-1-1:2005 Eurocode 3 – Design of steel structures – Part 1-1: general rules and rules for buildings; BSI, London, UK.
- Chitra Ganapathi, S., Annie Peter, J., Lakshmanan, N. and Iyer, N.R. (2016), “Behavior of light weight sandwich panels under out of plane bending loading”, *Steel Compos. Struct., Int. J.*, **21**(4), 775-789.
- Choi, J.Y., Park, Y.G., Choi, E.S. and Choi, J.H. (2010), “Applying precast slab panel track to replace timber track in an existing steel plate girder railway bridge”, *Proceedings of the Institution of Mechanical Engineers, Part F: Journal of Rail and Rapid Transit*, **224**(3), 159-167.
- Chopra, A.K. (2011), *Dynamics of Structures – Theory and Applications to Earthquake Engineering*, (4th Edn.), Prentice Hall, Upper Saddle River, NJ, USA.
- Dassault, (2012), ABAQUS theory manual; Available at: https://things.maths.cam.ac.uk/computing/software/abaqus_docs/docs/v6.12/books/stm/default.htm (Accessed on 1st August 2016)
- De Silva, S. and Thambiratnam, D.P. (2011), “Vibration characteristics of concrete-steel composite floor structures”, *ACI Struct. J.*, **108**(6), 1-9.
- Ding, X., Fan, Y., Kong, G. and Zheng, C. (2014), “Wave propagation in a concrete filled steel tubular column due to transient impact load”, *Steel Compos. Struct., Int. J.*, **17**(6), 907-927.
- El-Dardiry, E. and Ji, T. (2006), “Modelling of the dynamic behaviour of profiled composite floors”, *Eng. Struct.*, **28**(4), 567-579.
- Esveld, C. (1997), “Low-maintenance ballastless track structures”, *Rail Eng. Int. Ed.*, **26**(3), 13-16.
- Fang, G., Wang, J., Li, S. and Zhang, S. (2016), “Dynamic characteristics analysis of partial-interaction composite continuous beams”, *Steel Compos. Struct., Int. J.*, **21**(1), 195-216.
- Feldmann, M., Heinemeyer, C. Butz, C., Caetano, E., Cunha, A., Galanti, F., Goldack, A., Hechler, O. Hicks, S., Keil, A., Lukic, M., Obiala, R., Shlaich, M., Sedlacek, G., Smith, A. and Waarts, P. (2009), “Design of floor structures for human induced vibrations”, Office of the official publications of the European Communities, Luxembourg.
- Freudenstein, S. (2010), “RHEDA 2000®: Ballastless track systems for high-speed rail applications”, *Int. J. Pavement Eng.*, **11**(4), 293-300
- Griffin, D.W.P. (2013), “Design of precast concrete steel-concrete panels for track support: For use on the Sydney Harbour Bridge”, Honour Thesis; University of Western Sydney, Kingswood, Australia.
- Griffin, D.W.P., Mirza, O., Kwok, K. and Kaewunruen, S. (2014), “Composite slabs for railway construction and maintenance: a mechanistic review”, *The IES J. Part A: Civil & Struct. Eng.*, **7**(4), 243-262.
- Griffin, D.W.P., Mirza, O., Kwok, K. and Kaewunruen, S. (2015), “Finite element modelling of modular precast composites for railway track support structure: A battle to save Sydney Harbour Bridge”, *Aust. J. Struct. Eng.*, **16**(2), 150-168.
- Hou, Z., Xia, H., Wang, Y., Zhang, Y. and Zhang, T. (2015), “Dynamic analysis and model test on steel-concrete composite beams under moving loads”, *Steel Compos. Struct., Int. J.*, **18**(3), 565-582.
- Kaewunruen, S. (2014), “Monitoring in-service performance of fibre-reinforced foamed urethane material as timber-replacement sleepers/bearers in railway urban turnout systems”, *Struct. Monitor. Maintenance*, **1**(1), 131-157. [Invited]
- Kaewunruen, S., Remennikov, A.M. and Murray, M.H. (2014), “Introducing limit states design concept to concrete sleepers: an Australian experience”, *Frontiers Mat.*, **1**(8), 1-3.
- Kar, V.R. and Panda, S.K. (2015), “Nonlinear flexural vibration of shear deformable functionally graded spherical shell panel”, *Steel Compos. Struct., Int. J.*, **18**(3), 693-709.
- Kimani, S.K. (2016), “Free vibration analysis of precast steel-concrete composite slab panel for track support: Finite Element Method”, M.Sc. Thesis; School of Engineering, University of Birmingham, Birmingham, UK, 70 p.
- Kim, H.Y. and Jeong, Y.J. (2006), “Experimental investigation on behaviour of steel-concrete composite bridge decks with perfbond ribs”, *J. Constr. Steel Res.*, **62**(5), 463-471.
- Kim, H.Y. and Jeong, Y.J. (2009), “Steel-concrete composite bridge deck slab with profiled sheeting”, *J. Constr. Steel Res.*, **65**(8), 1751-1762.
- Kim, H.Y. and Jeong, Y.J. (2010), “Ultimate strength of a steel-concrete composite bridge deck slab with profiled sheeting”, *Eng. Struct.*, **32**(2), 534-546.
- Lam, D. and El-Lobody, E. (2001), “Finite element modelling of headed stud shear connectors in steel-concrete composite beam”, (A. Zingoni Ed.), *Struct. Eng., Mech. Compos.*, Elsevier Science, Oxford, UK, pp. 401-408.
- Lezgy-Nazargah, M. and Kafi, L. (2015), “Analysis of composite steel-concrete beams using a refined high-order beam theory”, *Steel Compos. Struct., Int. J.*, **18**(6), 1369-1389.
- Manalo, A., Aravinthan, T., Karunasena, W. and Ticoalu, A. (2010), “A review of alternative materials for replacing existing timber sleepers”, *Compos. Struct.*, **92**(3), 603-611.
- Mashhadi, J. and Saffari, H. (2016), “Effects of damping ratio on dynamic increase factor in progressive collapse”, *Steel Compos. Struct., Int. J.*, **22**(3), 677-690.
- Matias, S. (2015), “Numerical modelling and design of slab tracks - Comparison with ballasted tracks”, University of Lisbon, Portugal.
- Max Bogl, FFB slab track BOGL. Available at: <https://max-boegl.de/en> (Accessed on 1st July 2016)
- Mello, A.V.de A., da Silva, J.G.S., Vellasco, P.C.G.da S., de Andrade, S.A.L. and de Lima, L.R.O. (2008), “Modal analysis of orthotropic composite floors slabs with profiled steel decks”, *Latin Am. J. Solids Struct.*, **5**(1), 47-73.
- Michas, G. (2012), “Slab track systems for high-speed railways”, Master Degree Project, Royal Institute of Technology, Sweden.
- Mirza, O., Kaewunruen, S., Kwok, K. and Giffins, D. (2016), “Design and modelling of pre-cast steel-concrete composites for resilient railway track slabs”, *Steel Compos. Struct., Int. J.*, **22**(3), 537-565.
- Moon, J., Ko, H.J., Hyun Sung, I. and Lee, H-E. (2015), “Natural frequency of a composite girder with corrugated steel web”, *Steel Compos. Struct., Int. J.*, **18**(1), 255-271.
- Peng, D., Wei, Z. and Liu, J. (2012), “The exploration and research of CRTS I slab ballastless track used in the freight lines”, *Appl. Mech. Mater.*, **253**, 2031-2034.
- Perkins, N.C. and Mote, Jr. (1986), “Comments on curve veering in eigenvalue problems”, *J. Sound Vib.*, **106**(3), 451-463.
- Remennikov, A.M. and Kaewunruen, S. (2008), “A review of loading conditions for railway track structures due to train and track vertical interaction”, *Struct. Control Health Monitor.*, **15**(2), 207-234.
- Remennikov, A.M., Murray, M.H. and Kaewunruen, S. (2012), “Reliability based conversion of a structural design code for

- prestressed concrete sleepers”, *Proceedings of the Institution of Mechanical Engineers, Part F: Journal of Rail and Rapid Transit*, **226**(2), 155-173.
- Remennikov, A.M. and Kaewunruen, S. (2014), “Experimental load rating of aged railway concrete sleepers”, *Eng. Struct.*, **76**(10), 147-162.
- Robertson, I., Masson, C., Sedran, T., Barresi, F., Caillau, J., Keseljevic, C. and Vanzenberg, J.M. (2015), “Advantages of a new ballastless track form”, *Constr. Build. Mater.*, **92**, 16-22.
- Shim, C.S., Lee, P.G. and Chang, S.P. (2001), “Design of shear connection in composite steel and concrete bridges with precast decks”, *J. Constr. Steel Res.*, **57**, 203-219.
- Smith, A.L., Hicks, S.J. and Devine, P.J. (2009), *Design of Floors for Vibration: A New Approach*, The Steel Construction Institute, Ascot, Berkshire, UK.
- Sugimoto, I., Yoshida, Y. and Tanikaga, A. (2013), “Development of composite steel girder and concrete slab method for renovations of existing steel railway bridges”, *Quarterly Report of RTRI*, **54**(1), pp.1-11.
- Tindall, P. (2008), ‘Aluminium in bridges’, In: ICE manual of bridge engineering, (G. Parke and N. Hewson Eds.), (2nd Edn.) Thomas Telford, pp. 345-355, London, UK.
- Venghiac, V.M. and D’Mello, C. (2010), “The influence of the thickness of the slab and concrete grade on composite floors”, *Buletinul Institutului Politehnic din Iasi. Sectia Constructii, Arhitectura*, **56**(2), p. 85.

DL